The Fabrication of Sub-micron Size Cesium Iodide X-Ray Scintillator

Chien Wan Hun[a], Po Chun Chen[b], Ker Jer Huang[c], Chien Chon Chen[*d]
[a]Department of Mechanical Engineering, National United University, Miaoli 36003, Taiwan; [b]Medical Electronic System Research Laboratory, National Chiao Tung University, Hsinchu 30010,Taiwan; [d]Department of Energy Engineering, National United University, Miaoli 36003, Taiwan; [c]Chung-Shan Institute of Science and Technology, Taoyuan 325, Taiwan

ABSTRACT

The cesium iodide (CsI) scintillator can converts incident X-ray into visible light with very high conversion efficiency of optical photons. The incident energy, response time, film thickness, sample size, and spatial resolution require in engineering and medical applications are difference. A smooth and flat surface and single crystal structure of CsI enhance the X-ray to visible light conversion. However, the regular CsI is soft and extremely hygroscopic; it is very difficult to polish to obtain a smooth and optical flat plane. In order to obtain a good quality of CsI scintillator for X-ray application we used an ordering channel as template and formed sub-micron CsI wire in the template. The fabrication process including: (1) Ordering structure of nano or sub-micron channels were made by an anodization method; (2) fill CsI scintillated film on the channel by CsI solution, (3) fill CsI melt into the channel formation single crystal of sub-micron crystalline scintillator after solidification. The non-vacuum processes of anodization and solidication methods were used for the sub-micron CsI scintillator column formation that is cost down the scintillator fabrication. In addition, through the fabrication method, the ordering structure scintillator of scintillator can be made by anodic treatment and die casting technology with low cost and rapid production; moreover, the film oxidized metal tubes of the tubular template can be further manufactured to nano tubes by adjusting electrolyte composition, electrolysis voltage, and processing time of anodic treatment, and the aperture size, the thickness and the vessel density of the nano tube can be controlled and ranged from 10 nm to 500 nm, 0.1 μm to 1000 μm, and hundred million to thousand billion tube/cm^2, respectively.

Keywords: cesium iodide, X-ray, scintillator, template

1. INTRODUCTION

In an X-ray detector assembly, an amorphous silicon detector substrate is coated with a vapor phase deposited X-ray scintillator material. The scintillator material generates photons isotropically from the absorption of the X-rays. Scintillator is a product of high-energy physics technology, which is used for transforming X-ray to an electronic signal or a visible light; therefore, the visible light transformed from X-ray can be further converted to an electronic signal by conventional optics device, for example, charge-coupled device (CCD). The scintillation occurring in the scintillator is a fluorescence induced by radiation. When a high-energy wave irradiates the scintillator, the ground state electrons in the scintillator would be excited and then migrate from ground state to excited state. Therefore, those excited electrons can further migrate to light-emitting excited state through non-light-emitting way, and then decay to lower energy state or base state for emitting photons (400~1100 nm).[1-3]

Since crystalline scintillator includes high energy gap, the photons still cannot be effectively emitted although large electrons in conduction band migrate to valence band, or, the emitted photons cannot become visible light due to their high energy. Therefore, for increasing the emitting efficiency of visible light, a small amount of the activator is doped into crystalline scintillator for reducing the energy gap. [4, 5]

Because scintillator is able to transform X-ray to visible light, it is widely applied in medical equipments, nuclear medicine, and security detection technologies. Currently, Scintillators are divided into CsI scintillator, CsI(Na) scintillator and CsI(Tl) scintillator, wherein the CsI scintillator has been became the most conventionally used scintillator for its advantages of easy to be process, large size, sensitive to radiation, and high light-emitting efficiency. Generally, a good scintillator includes the following properties: (1) transforming a radiation wave to a

Thermosense: Thermal Infrared Applications XXXVII, edited by Sheng-Jen (Tony) Hsieh, Joseph N. Zalameda,
Proc. of SPIE Vol. 9485, 94850M · © 2015 SPIE · CCC code: 0277-786X/15/$18 · doi: 10.1117/12.2176785

detectable light by high scintillation effect; (2) linear transform; (3) the production of the detectable light is proportional to energy of the radiation wave; (4) including transparency and low self-radioactivity; and (5) short light-decaying time. [6, 7]

Moreover, various application fields demand different requirements to the scintillators on incident radiation energy (keV), reaction time (ms), thickness (μm), area (cm^2), and spatial resolution (1 p/mm). for example, crystallography:8–20 (keV), <0.5 (ms), 30–50(μm), 30×30 (cm^2), 10 (lp/mm); mammography: 20–30 (keV), <0.1 (ms), 100–150 (μm), 20×25 (cm^2), 15-20 (lp/mm); dental Imaging: 50–70 (keV), <1 (ms), 70–120 (μm), 2.5×3.5 (cm^2), 7-10 (lp/mm); nondestructive testing: 30–400 (keV), <0.1 (ms), 70–1000 (μm), 10×10 (cm^2), 5-10 (lp/mm); and Astronomy: 30–600 (keV), <0.05 (ms), 70–2000 (μm), 30×30 (cm^2), 4-5 (lp/mm), the detail physical characterizations of scintillator is in the table 1 [8-12].

Table 1. The physical properties of NaI(Ti), CsI(Ti), and CsI(Na) scintillation crystals.

Chemical formula	NaI (Tl)	CsI (Tl)	CsI (Na)
Density, g/cm^3	3.67	4.51	4.51
Melting point, ℃	651	621	621
Maximum wavelength (λ_{max}), nm	410	560	420
Refraction Index at λ_{max}	1.85	1.84	1.84
Relative amount of light output, %	100	45	85
Output light amount, Photon/MeV	4.1-5.0 x 10^4	4.5-5.1 x 10^4	3.5-4.2 x 10^4
Decay time, ms	0.23	1.0	0.63
Afterglow (after 6 ms), %	0.5-5.0	0.5-5.0	0.5-5.0
Background , pulse/sec/kg	≦ 3.0	≦ 3.0	≦ 3.0

In addition, anodic treatment is conventionally applied in surface corrosion resistance, painting, electrical insulation, electroplating, and wear resistance. The anodic oxide film made by anodic treatment usually includes porous-structure, therefore a post sealing process must be applied to the anodic oxide film for facilitating the anodic oxide film become a dense membrane. Anodic treatment has the advantages of low cost and rapid production, and capable of being applied in producing large area products, such as dye-sensitized solar cells, thermal conductive sheets and thermal insulating components. Besides the anodic treatment, die casting process is also a low cost, rapid production technology.

The template of anodic aluminum oxide (AAO) is a type of ceramic with a high melting point (2072 °C) and hardness (9 on the Mohs scale of mineral hardness). Anodic alumina has been named differently, such as anodic aluminum oxide (AAO) [13-17], anodic alumina nanoholes (AAN) [18], anodic alumina membrane (AAM) [19, 20], or porous anodic alumina (PAA) [21]. The anodic oxide film consists of two layers: the outer porous thick layer and the inner thin layer, which is dense and dielectrically compact, and thus it is called as the barrier layer or dielectric layer. The barrier layer thickness is typical between 0.1 and 2% of that of the entire film [22]. Depending on the electrolytes, anodizing time and voltage, AAO could be formed as compact alumina, thick porous alumina, or etching types. Compact alumina (no pores) is formed in a very weak acid or neutral solution, and its thickness is determined by the applied voltage. Thick porous alumina forms in a medium-strength acid solution, and its thickness is determined by the anodizing time, pore density increases when anodizing time increases, but decreases when higher anodizing voltage, lower electrolyte temperature (hard coating). For etching alumina formed in strong acid or basic solutions, the thickness is determined by the diffusion limits of electrolyte, and the pore density increases when the anodizing time increases. It is generally accepted that the thickness of barrier-type alumina is mainly determined by the applied voltage (1~1.4 nm/V) [23], even though there are slight deviations depending on the electrolytes and temperature. The maximum attainable thickness in the barrier-type alumina film was reported to be less than 1 μm, corresponding to the breakdown voltage in the range of 500~700 V (DC) [24-26]. Akahori [27] has demonstrated that the melting point of this inner oxide layer is 1000 ・ C, also the AAO template is stable around 800 ℃ [28], which is much lower than that of the bulk alumina.

On the other hand, traditional CsI scintillator process would cause some drawbacks in the CsI scintillator, for example, yellow discoloration, air pores, cloudiness, etc., and the yellow discoloration, the air pores and the cloudiness would impact the output of visible light and further reduce the efficiency of the CsI scintillator. In scintillator, the yellow discoloration is resulted from the combination of oxygen ions and thallium ions in the surface

of scintillator, the air pores are caused by air or impurity remaining in the scintillator, and the cloudiness is an atomization induced by gathering of small oxygen bubbles.

According to the traditional CsI scintillator process includes many drawbacks, the semiconductor process technologies are used for manufacturing the scintillators, which includes the steps of: firstly, forming micron tube array on a silicon substrate by way of deep reactive ion etching (DRIE) or laser drilling, wherein the micron tube array is used as a waveguide film, and includes an aspect ratio of 20˜25 and a tube diameter of few microns. Next, vapor (or liquid) deposition is used for filling CsI material into the micron tube array, so as to complete a CsI scintillator. However, the mask, lithography, exposure, etching, and crystal growth equipment adopted in semiconductor process technology result in high manufacturing time and cost to CsI scintillator.

Accordingly, in view of the traditional CsI scintillator process and the semiconductor process technology for making CsI scintillator still have shortcomings and drawbacks, the inventor of the present application has made great efforts to make research and eventually provided a scintillator with sub-micron column structure and a manufacturing method, wherein the anodic treatment and the die casting technology having the advantages of low cost and rapid production are utilized for manufacturing a high-value scintillator with sub-micron column structure, and this scintillator with sub-micron column structure can also be applied in medical equipment, nuclear medicine, and security detection technologies.

2. THE CESIUM IODIDE FABRICATION PROCESS AND CHARACTERIZATIONS

The experimental procedure included AAO template fabrication and CsI sub-micron column fabrication. The experiment steps are:

(1) Fabricating a tubular template having a thin film oxidized metal tubes by processing an anodic treatment.
(2) Adjusting the tube diameter of the thin film oxidized metal tubes by a chemical etching process.
(3) Forming a thin film scintillator on the inner walls of the thin film oxidized metal tubes by a chemical impregnation process.
(4) Filling a liquid phase of scintillator material into the thin film oxidized metal tubes by a die casting process; so as to form a scintillator column in each thin film oxidized metal tube.

The high quality AAO template fabrication steps are: Al foil (99.999%) → mechanical-polishing → annealing → electro-polishing → 1st anodization → remove AAO → 2nd anodization → remove aluminum substrate → remove barrier layer → both sides pore widening. the detail experimental operation and parameters as discuss in the following.

The AAO quality was depended on the purity of Al substrate. A higher Al purity for example, 99.999% (5N) a higher quality AAO with uniform pore diameter can be obtained. However; the 5N Al foil is expensive on the marked. In order to have a various thickness and cheap Al foil we rolled bulk Al to Al foil by a rolling machine (Figure 1). The staring from 2 cm thickness bulk Al to 0.3 mm Al foil which has a uniform thickness pure Al grains of microstructure.

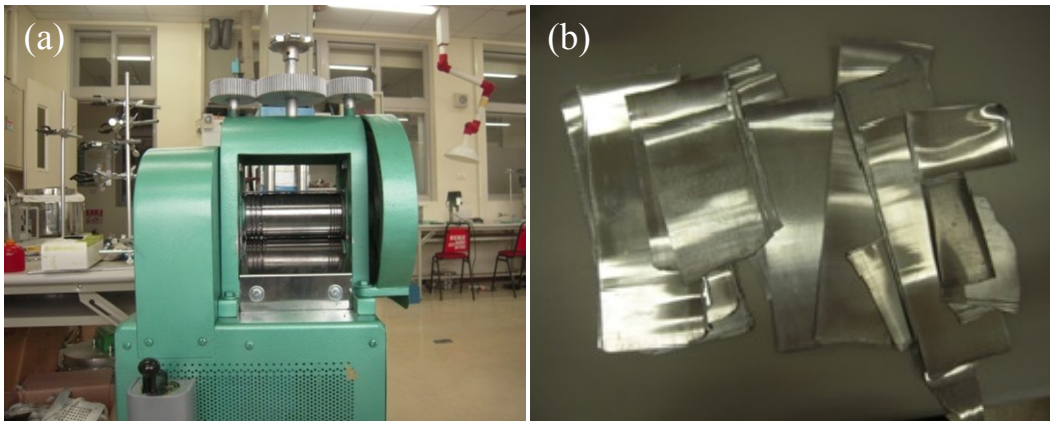

Figure 1. The Al foil was rolled form Al bulk by a rolling machine; (a) rolling machine, (b) Al foil.

The AAO templates with 15 nm, 60 nm, and 400 nm diameters were generated by anodizing a pure aluminum

(Al) substrate (99.999%) in acid solutions of sulfuric acid (H_2SO_4), oxalic acid $(COOH)_2$ or phosphoric acid (H_3PO_4). The Al substrate was first grind to #1000 by SiC water proof paper then annealing in the air furnace at 550℃ for 1 hr. The sample was then electro-polished in a bath consisting of 15 vol.% perchloric acid ($HClO_4$, 70%), 70 vol.% ethanol (C_2H_6O, 99.5%) and 15 vol.% monobutylether ($(CH_3(CH_2)_3OCH_2CH_2OH)$, 85%) applied 42 volt (DC) for 10 min, used platinum plate as a counter. The 15 nm pore diameter template was then fabricated by anodizing the polished Al substrate at 18V in 10 vol.% H_2SO_4 at 15℃ for 20 min which is called the first anodization. In order to obtain an order pattern on the substrate for the second anodization, the first anodization film was removed in the 1.8 wt.% chromic acid (CrO_3) + 6 vol.% H_3PO_4 solution at 60℃ for 40 min.

The substrate with regular pattern on the surface was used for the second anodization for several hours to form a various AAO film thickness. The Al substrate can be remove when the sample was put in a saturated copper chloride ($CuCl_2$) + 10 vol.% hydrochloric acid (HCl) for 30 min. Finally put the sample in the 5 vol.% H_3PO_4 at 25 ℃ for 20 min a nanotubes were widened to a ordering array and a good quality AAO film forming. As same as the above process, for 60 nm pore diameter AAO template, the electrolyte is 3 vol.% $(COOH)_2$ at 25℃, and applied voltage is 40 V, the time of pore widening is 90 min. And for 400 nm pore diameter AAO template, the electrolyte is 1 vol.% H_3PO_4 at 0℃, and applied voltage is 200 V, the time of pore widening is 120 min [29]. Figure 2 showed the AAOs have nano-pore of 10 nm and the sub-micron pore of 357 nm structure. The ordering pores which can be a host or template for the assistance of CsI wire or column fabrication.

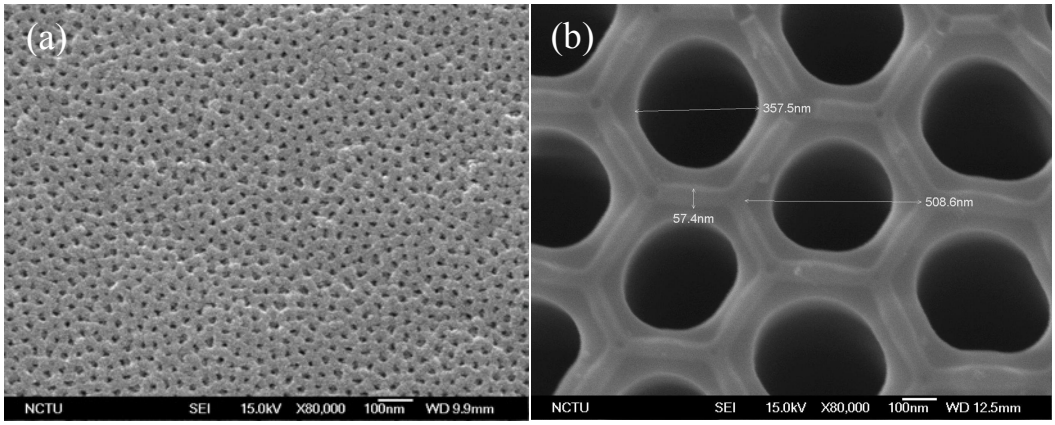

Figure 2. SEM images of AAO template. (a) AAO with pore diameter of 10 nm by 10 vol.% H_2O_4 electrolyte at 18V anodization, (b) AAO with pore diameter of 357 nm by 1.5 vol.% H_3PO_4 electrolyte at 180V anodization.

Figure 3 showed the process of cesium iodide (sodium) tablet formation by vacuum melting and ingot-making process. (a) The 1: 0.3 mole ratio of sodium iodide (NaI) : cesium iodide(CsI) powder are into the quartz tube. (b) In order to avoid volatilization during melting of iodine vapor pressure over the case of the tube caused by explosion of a quartz tube, the quartz tube is the use of a mechanical pump to maintain the pressure inside the pipe within the range of 10-1 ~ 10^{-2} torr. (c) Because the melting point of CsI and NaI are 621 ℃ and 651 ℃ the available butane burner can melt the mixture powders. (d) The use of the mixed powder is heated torch for about 10 seconds after the visible a red solution in a quartz tube, in order to avoid the loss of iodine vapor heating and melt mixing the shaking time should be controlled within 30 seconds. (e) Removed the heater and closed the vacuum valve on the quartz tube the melt can naturally solidify to a NaI/CsI solid. (f) wait for the iodine vapor (boiling point: 184 ℃) and iodine drops (boiling point: 113 ℃) stable in the quartz tube. (g) Break out the tube and get the solid NaI/CsI. (h) the use of an agate mortar rod cesium iodide / sodium iodide ground into a powder, and the powder into a mold to tungsten steel spindles hydraulic machine plus 100 kgf / cm^2, holding pressure 0.5 min of spindles. (i) Finally, cesium iodide / sodium iodide tablets were placed in a quartz tube at 400 ℃ for 8h forming a homogeneous NaI/CsI tablet.

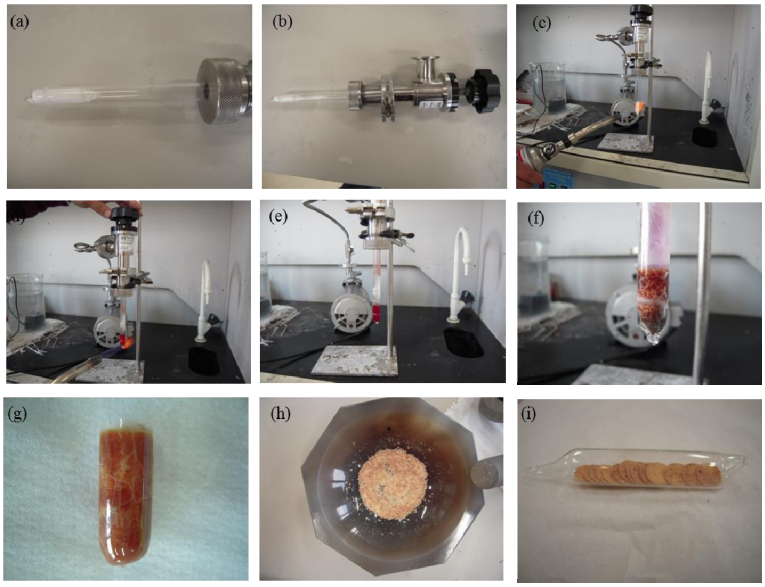

Figure 3. the CsI (Na) powder fabrication by the vacuum melting process; (a) CsI/ NaI mixture powder in a quartz tube, (b)quartz tube in a vacuum state , (c) heating the vacuuming quartz tube which CsI/ NaI mixture powder has inside ,(d) CsI/ NaI mixture melt forming, (e) cooling the melt, (f) solid CsI/ NaI mixture compound forming, (g) remove the CsI/ NaI mixture compound from the quartz tube, (h) homogeneous CsI/ NaI powder forming, (i) homogeneous CsI/ NaI tablet forming.

Figure 4 showed the CsI (Na) tablet formation by a uniaxial compressive method; (a) homogeneous CsI/ NaI powder in a mold, (b) the mold with CsI/ NaI powder inside on a compressive mechane, (c) CsI/ NaI sheet forming, (d) NaI sheet on an AAO surface. CsI sub-micron column fabrication steps are: the starting materials are CsI powder, NaI powder, and high-purity Al foil. The Al foil was then through anodization formation AAO template. And, 1 mole CsI + 0.03 mole NaI mixing powder was then through shaping and sintering formation CsI (Na) ingot. In order to observe the CsI (Na) column inside AAO template the following experiment steps were needed. (1) CsI (Na) ingot put on the AAO surface, (2) heating CsI (Na)/AAO at 630 °C, applied a hydraulic pressure (10 kgf/cm^2) to the CsI (Na) melt, (3) cooling CsI (Na)/AAO sample at 30 °C/min of cooling rate. According to above steps we can obtain the CsI (Na) nano or sub-micron CsI (Na) column [30-32].

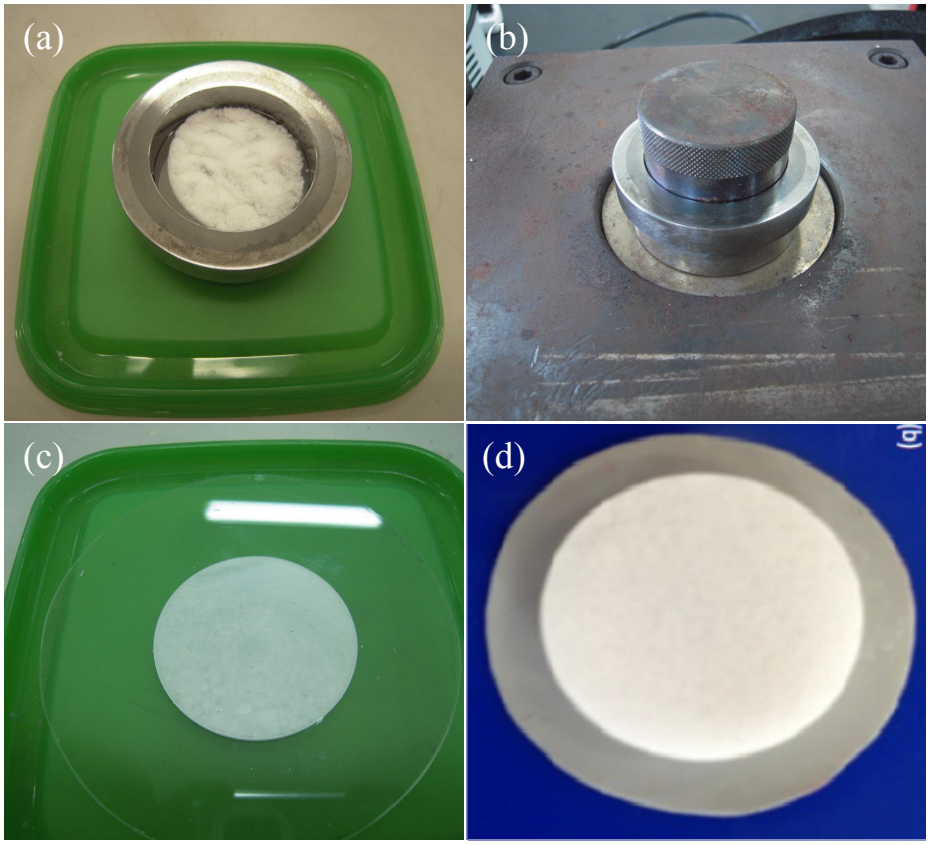

Figure 4. CsI (Na) tablet formation by a uniaxial compressive method; (a) homogeneous CsI/ NaI powder in a mold, (b) the mold with CsI/ NaI powder inside on a compressive mechane, (c) CsI/ NaI sheet forming, (d) NaI sheet on an AAO surface.

We also compared the quality and microstructure of CsI columns that formed under normal pressures of 1 atm and applied pressure of 10 kgf/cm^2. When the CsI/AAO sample was under a lower pressure at high temperature, large amounts of $CsI_{(g)}$, $I_{2(g)}$, and $CsO_{x(g)}$ vapors were produced on and in the AAO, so not enough CsI melted on the AAO surface, leading to discontinuous CsI columns inside the AAO template. For example, Figure 5 showed SEM images of CsI columns inside AAO at 1 atm and 650℃ experimental conditions with poor CsI filling in the AAO template. (a) Top view of partial CsI columns inside AAO, (b) side view image of partial and discontinue CsI columns inside AAO. However, when the CsI/AAO sample was under a higher pressure at high temperature, the $CsI_{(g)}$, $I_{2(g)}$, and $CsO_{x(g)}$ vapors can be reduced; therefore, a continue and high filling ratio of CsI in AAO can be obtained. For example, figure 6 shows SEM images of CsI columns with good filling of the AAO template, produced under pressure of 10 kgf/cm^2 at 630ºC. The applied pressure to the casting mold that assisted to the CsI melts into AAO template and form CsI column.

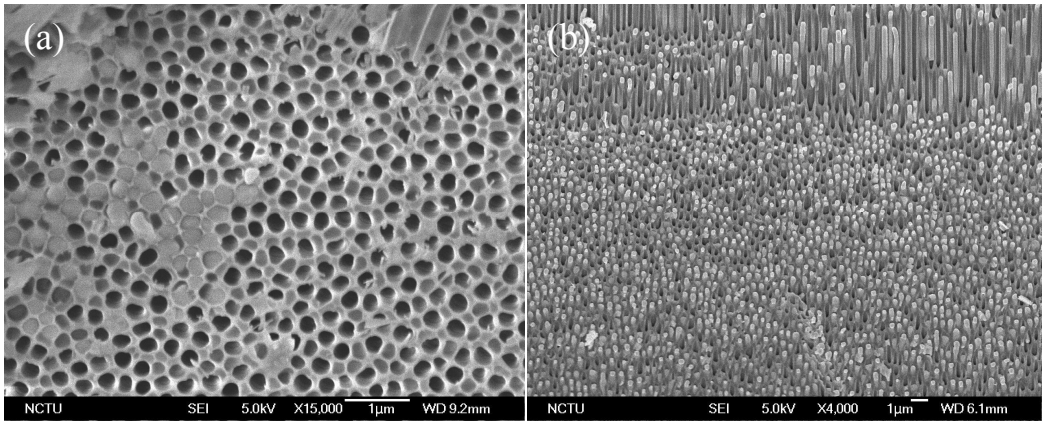

Figure 5. SEM images of CsI columns inside AAO at 1 atm and 650℃ experimental conditions with poor CsI filling in the AAO template. (a) Top view of partial CsI columns inside AAO, (b) side view image of partial and discontinue CsI columns inside AAO.

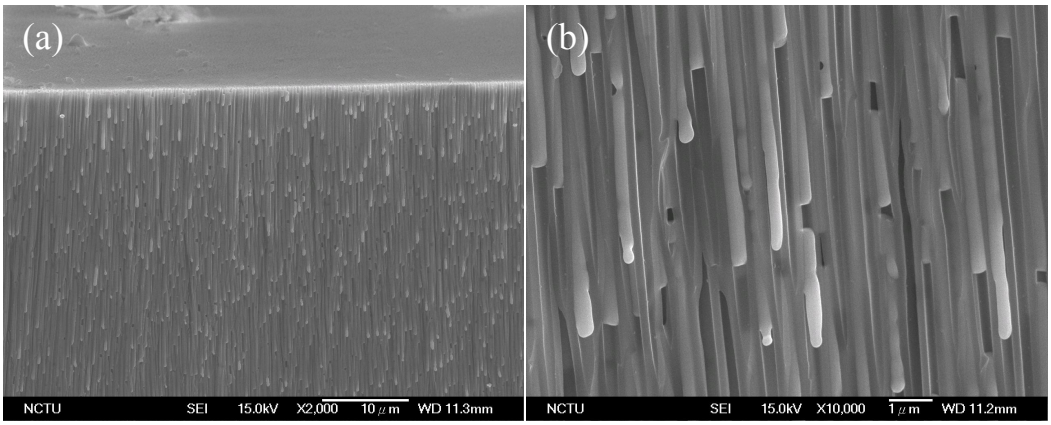

Figure 6. SEM side view image of CsI columns inside AAO at 10 atm and 650℃ experimental conditions with well CsI filling in the AAO template. (a) Lower magnification image, (b) Higher magnification image.

3. CONCLUSIONS

In this paper we have been clearly and completely introduced the scintillator with sub-micron column structure and the manufacturing method. In summary, the fabrication method of sub-micron column CsI has the following advantages:

1. It utilizes anodic treatment and die casting technology with low cost and rapid production to manufacture a high-value scintillator with sub-micron column structure, and this scintillator with sub-micron column structure can also be manufactured by mass production.
2. By using the manufacturing method, the scintillator with sub-micron column structure or nano-column structure can be made for being applied in medical equipment, nuclear medicine, and security detection technologies.
3. The AAO template can be further manufactured to nano-tubes by adjusting electrolyte composition, electrolysis voltage, and processing time of anodic treatment, and the aperture size, the thickness and the vessel density of the nano-tube can be controlled and ranged from 10 nm to 500 nm, 0.1 μm to 1000 μm, and 10^8 to 10^{12} tube/cm^2, respectively.

ACKNOWLEDGEMENTS

This work was financially supported by the Chung-Shan Institute of Science and Technology (CSIST) under the Contract No. CSIST-104-EC-17-A-22-0442 and, National Science Council, Taiwan under the Contract No. 103-2221-E-239-004.

REFERENCES

[1] M. Stampanoni, G. Borchert, P. W., R. Abela, B. Patterson, S. Hunt, D. Vermeulen,.P. Rüegsegger, "High resolution X-ray detector for synchrotron-based microtomography", Nuclear Instruments and Methods in Physics Research Section A: Accelerators, Spectrometers, Detectors and Associated Equipment 491, 291-301 (2002).

[2] A. Ananenko, A. Fedorov, A. Lebedinsky, P. Mateychenko, V. Tarasov, Y. Vidaj, "structural dependence of CsI(Tl) film scintillation properties", Semiconductor Physics, Quantum Electronics & Optoelectronics 7, 297-300 (2004).

[3] E. Zych, C. Brecher, and H. Lingertat, Depletion of high-energy carriers in YAG optical ceramic materials, Spectrochimica Acta Part A: Molecular and Biomolecular Spectroscopy 54, 1771-1777 (1998).

[4] M. Stampanoni, G. Borchert, P. W., R. Abela, B. Patterson, S. Hunt, D. Vermeulen,.P. Rüegsegger, "High resolution X-ray detector for synchrotron-based microtomography", Nuclear Instruments and Methods in Physics Research Section A: Accelerators, Spectrometers, Detectors and Associated Equipment 491, 291-301 (2002).

[5] A. Ananenko, A. Fedorov, A. Lebedinsky, P. Mateychenko, V. Tarasov, Y. Vidaj, "structural dependence of CsI(Tl) film scintillation properties", Semiconductor Physics, Quantum Electronics & Optoelectronics 7, 297-300 (2004).

[6] A. M. Gurvich, "Luminescent screens for mammography", Radiation Measurements 24, 325-330 (1995).

[7] A Koch, H Rosenfeldt, "Powder-phosphor screens combined with interference filters for X-ray imaging with increased brightness", Nuclear Instruments and Methods in Physics Research Section A: Accelerators, Spectrometers, Detectors and Associated Equipment 432, 358-363 (1999).

[8] U.L. Olsen, X. Badel, J. Linnros, M. Di Michiel, T. Martin, S. Schmidt, H.F. Poulsen, "Development of a high-efficiency high-resolution imaging detector for 30–80 keV X-rays", Nuclear Instruments and Methods in Physics Research Section A 576, 52-55 (2007).

[9] C.M. Schaefer-Prokop, D.W. De Boo, M. Uffmann, M. Prokop. DR and CR, "Recent advances in technology", European Journal of Radiology 72, 194-201(2009).

[10] A. Koch, C. Raven, P. Spanne, A. Snigirev, "X-ray imaging with submicrometer resolution employing transparent luminescent screens", Journal of the Optical Society of America A 15, 1940-1951 (1998).

[11] S Zazubovich. Physics of halide scintillators, Radiation Measurements 33, 699-704 (2001).

[12] U.L. Olsen, X. Badel, J. Linnros, M. Di Michiel, T. Martin, S. Schmidt, H.F. Poulsen, Development of a high-efficiency high-resolution imaging detector for 30–80 keV X-rays, Nuclear Instruments and Methods in Physics Research Section A: Accelerators, Spectrometers, Detectors and Associated Equipment 576, 52-55 (2007).

[13] Wood GC, O'Sullivan JP, "The Anodizing of Aluminum in Sulphate Solutions", Electrochim. Acta 15, 1865-1876 (1970).

[14] Xing H, Zhiyuan L, Kai W, Yi L, "Fabrication of Three Dimensional Interconnected Porous Carbons from Branched Anodic Aluminum Oxide Template", Electrochem. Comm. 13, 1082-1085 (2011).

[15] Wood GC, Skeldon P, Thompson GE, Shimizu K, "A Model for the Incorporation of Electrolyte Species into Anodic Alumina", J. Electrochem. Soc. 143, 74-83 (1996).

[16] Comstock D. J. , Christensen S. T. , Elam J. W. , Pellin M. J. , Hersam M. C. , "Synthesis of Nanoporous Activated Iridium Oxide Flms by Anodized Aluminum Oxide Templated Atomic Layer Deposition", Electrochem. Comm. 12, 1543-1546 (2010).

[17] Ghahremaninezhad A., Asselin E., Dixon D. G. , "One-step Template-free Electrosynthesis of 300 μm Long Copper Sulfide Nanowires", Electrochem. Comm. 13, 12-15 (2011).

[18] T. Iwasaki, T. Motoi, Den T, Multiwalled, "Carbon Nanotubes Growth in Anodic Alumina Nanoholes", Appl. Phys, Lett. 75, 2044-2046 (1999).

[19] Pang Y. T., Meng G. W., Fang Q. , Zhang L. D. , "Silver Nanowire Array Infrared Polarizers", Nanotechnology 14, 20-24 (2003).

[20] Wang Y. W. , Meng G. W., Liang C. H. , Wang G. Z., Zhang L. D., "Magnetic Properties of Ordered Fe_xAg_{1-x} Nanowire Arrays Embedded in Anodic Alumina Membranes", Chem. Phys. Lett. 339, 174-178 (2001).

[21] Stoleru V. G. , Towe E. , 'Optical Properties of Nanometer-sized Gold Spheres and Rods Embedded in Anodic Alumina Matrices", Appl. Phys. Lett. 85, 5152-5154 (2004).
[22] Masuda H. , Fukuda K. , "Ordered Metal Nanohole Arrays Made by a Two-Step Replication of Honeycomb Structures of Anodic Alumina", Science 268 1466-1468 (1995).
[23] O'Sullivan J. P., Wood G. C., "The Morphology and Mechanism of Formation of Porous Anodic Films on Aluminum', Proc. Royal Soc. London A 317, 511-543 (1970).
[24] Diggle J. W., Downie T. C., Goulding C. W., "Anodic Oxide Films on Aluminum', Chem. Rev. 69, 365-405 (1969).
[25] Hunter M. S., Fowel P., "Determination of Barrier Layer Thickness of Anodic Oxide Coatings", J. Electrochem. Soc. 101, 481-485 (1954).
[26] Hunter M. S., Fowel P., "Factors Affecting the Formation of Anodic Oxide Coatings", J. Electrochem. Soc. 101, 514-519 (1954).
[27] Akahori H., "Electron Microscopic Study of Growing Mechanism of Aluminum Anodic Oxide Film", J Electron. Microsc 10, 175-185 (1961).
[28] Iwasaki T., Motoi T., Den T., "Multiwalled Carbon Nanotubes Growth in Anodic Alumina Nanoholes" Appl. Phys, Lett.75, 2044-2046(1999).
[29] C. C. Chen, D. Fang, Z. Luo, "Fabrication and Characterization of Highly-Ordered Valve-Metal Oxide Nanotubes and Their Derivative Nanostructures", Review in Nanoscience and Nanotechnology 1, 229-256 (2012).
[30] C. Y. Chen, S. H. Chen, C. C. Chen, J. S. Lin, "Using Positive Pressure to produce a Sub-micron Single-Crystal Column of Cesium Iodide (CsI) for Scintillator Formation", Materials Letters 148, 138-141 (2015).
[31] C. C. Chen, S. F. Chang, Z. Luo, "Anodic-aluminum-oxide template assisted fabrication of cesium iodide (CsI) scintillator Nanowires", Materials Letters 112, 190-193 (2013).
[32] C. C. Chen, C. M. Chu, C. J. Wang, C. Y. Chen, K. J. Huang, "The Fabrication of Scintillator Column by Hydraulic Pressure Injection Method", World Academy of Science, Engineering and Technology International Journal of Mathematical, Computational, Physical and Quantum Engineering 8, 792-795 (2014).